

A Comparison of the Behavior of ^{64}Cu -Acetate and ^{64}Cu -ATSM In Vitro and In Vivo

Rebekka Huetting^{*1}, Veerle Kersemans^{*2}, Bart Cornelissen², Matthew Tredwell¹, Kamila Hussien², Martin Christlieb², Antony D. Gee³, Jan Passchier⁴, Sean C. Smart², Jonathan R. Dilworth¹, Véronique Gouverneur¹, and Ruth J. Muschel²

¹Department of Chemistry, Chemistry Research Laboratory, University of Oxford, Oxford, United Kingdom; ²CRUK/MRC Gray Institute for Radiation Oncology and Biology, University of Oxford, Oxford, United Kingdom; ³Division of Imaging Sciences and Biomedical Engineering, King's College London, St. Thomas' Hospital, London, United Kingdom; and ⁴GlaxoSmithKline, Clinical Imaging Centre, Imperial College London, London, United Kingdom

^{64}Cu -diacetyl-bis(*N*⁴-methylthiosemicarbazone), ^{64}Cu -ATSM, continues to be investigated clinically as a PET agent both for delineation of tumor hypoxia and as an effective indicator of patient prognosis, but there are still aspects of the mechanism of action that are not fully understood. **Methods:** The retention of radioactivity in tumors after administration of ^{64}Cu -ATSM in vivo is substantially higher for tumors with a significant hypoxic fraction. This hypoxia-dependent retention is believed to involve the reduction of Cu-ATSM, followed by the loss of copper to cellular copper processing. To shed light on a possible role of copper metabolism in hypoxia targeting, we have compared ^{64}Cu retention in vitro and in vivo in CaNT and EMT6 cells or cancers after the administration of ^{64}Cu -ATSM or ^{64}Cu -acetate.

Results: In vivo in mice bearing CaNT or EMT6 tumors, biodistributions and dynamic PET data are broadly similar for ^{64}Cu -ATSM and ^{64}Cu -acetate. Copper retention in tumors at 15 min is higher after injection of ^{64}Cu -acetate than ^{64}Cu -ATSM, but similar values result at 2 and 16 h for both. Colocalization with hypoxia as measured by EF5 immunohistochemistry is evident for both at 16 h after administration but not at 15 min or 2 h. Interestingly, at 2 h tumor retention for ^{64}Cu -acetate and ^{64}Cu -ATSM, although not colocalizing with hypoxia, is reduced by similar amounts by increased tumor oxygenation due to inhalation of increased O_2 . In vitro, substantially less uptake is observed for ^{64}Cu -acetate, although this uptake had some hypoxia selectivity. Although ^{64}Cu -ATSM is stable in mouse serum alone, there is rapid disappearance of intact complex from the blood in vivo and comparable amounts of serum bound activity for both ^{64}Cu -ATSM and ^{64}Cu -acetate. **Conclusion:** That in vivo, in the EMT6 and CaNT tumors studied, the distribution of radiocopper from ^{64}Cu -ATSM in tumors essentially mirrors that of ^{64}Cu -acetate suggests that copper metabolism may also play a role in the mechanism of selectivity of Cu-ATSM.

Key Words: ^{64}Cu -ATSM; hypoxia; ^{64}Cu -acetate; copper metabolism

J Nucl Med 2014; 55:128–134

DOI: 10.2967/jnumed.113.119917

The critical role of hypoxia in tumor biology underscores the need for high-performance hypoxia-selective indicators. There are several candidates for clinical detection of tumor hypoxia using PET radiotracers (1). ^{64}Cu -ATSM is one of them and benefits from favorable tumor-to-blood ratios (>2) and fast clearance, allowing rapid PET imaging after administration. Moreover, retention of copper after administration of ^{64}Cu -ATSM has been shown to correlate with poor prognosis. Although this retention could be due to tumor hypoxia, there have been few correlations of copper retention with hypoxia in clinical studies by immunohistochemical studies or comparisons of Cu-ATSM with ^{18}F -fluoromisonidazole. Copper retention, therefore, may not necessarily be entirely due to hypoxia in all cases, particularly if short imaging times are used. This does not invalidate the proven use of Cu-ATSM as a prognosis agent because nonhypoxic copper retention may well reflect tumor aggressiveness.

Since Fujibayashi et al. first observed hypoxia-selective retention of radioactivity from ^{62}Cu -ATSM in an ex vivo rat heart model of ischemia (2), numerous reports confirmed its hypoxia selectivity in vitro (3,4). To date, there is a consensus that in vitro Cu-ATSM undergoes bioreductive trapping under hypoxic conditions. After cellular entry, Cu(II)-ATSM is reduced to an unstable Cu(I)-ATSM species, a process inducing dissociation of the metal complex and subsequent irreversible trapping of Cu(I) within the cellular copper metabolic processes (5).

However, the proposed mechanism for hypoxia selectivity might not be as straightforward as initially assumed. Experimental and in silico studies indicated that variables such as pH also influence the stability of the reduced Cu(I) species and affect the reduction, reoxidation, and ligand dissociation events (6–9). Although hypoxia selectivity for ^{64}Cu -ATSM is evident in vitro and in vivo, some more recent studies found that the relationship between oxygenation status and uptake and retention of ^{64}Cu -ATSM varied with cell and tumor line (10,11). The correlation of intratumoral ^{64}Cu distribution with nitroimidazole-based markers was also variable and time-dependent (12–14). This suggests that the strong correlation between retention of radiocopper from Cu-ATSM and poor treatment outcome observed in clinical studies may be governed by additional mechanisms other than tumor pO_2 (11,15–17).

Recent reports have noted that copper, administered as simple copper salts, is retained in tumors and suggest that this might be used for cancer detection (18–21). Because there is little uptake of

Received Jan. 12, 2013; revision accepted Jun. 17, 2013.

For correspondence or reprints contact: Ruth J. Muschel, CRUK/MRC Gray Institute for Radiation Oncology and Biology, University of Oxford, Old Rd. Campus, Oxford, OX3 7LJ United Kingdom.

E-mail: ruth.muschel@oncology.ox.ac.uk

*Contributed equally to this work.

Published online Dec. 12, 2013.

COPYRIGHT © 2014 by the Society of Nuclear Medicine and Molecular Imaging, Inc.

^{64}Cu -acetate by cells in tissue culture, the in vivo tumor uptake of ^{64}Cu -acetate or other copper salts has not been compared with that of ^{64}Cu -ATSM. To delineate the copper-processing component in Cu-ATSM accumulation, we have investigated the biodistribution of both ^{64}Cu -ATSM and ^{64}Cu -acetate in CaNT and EMT6 tumors. In part, we selected ^{64}Cu -acetate as a control because we fully expected it, based on published cell uptake studies, to display no hypoxia selectivity and serve solely as a marker of the cellular copper-processing pool. We found that in vivo the retention of ^{64}Cu for ^{64}Cu -ATSM was broadly similar to that for ^{64}Cu -acetate, both at earlier and later times after administration. We further examined the intratumoral distribution and oxygen-dependence of uptake for both tracers. An initial comparison of the in vitro and in vivo speciation of ^{64}Cu -ATSM suggests that dissociation of ^{64}Cu -ATSM in vivo may in part be responsible for the similar behavior of ^{64}Cu -ATSM and ^{64}Cu -acetate.

MATERIALS AND METHODS

Radiochemical Synthesis

H_2ATSM was synthesized as previously reported (additional information is given in the supplemental data; supplemental materials are available at <http://jnm.snmjournals.org>).

^{64}Cu -ATSM (90% isolated radiochemical yield; >98% radiochemical purity) was prepared by reaction of the bis(thiosemicarbazone) proligand with ^{64}Cu -acetate (100–150 MBq) using reported procedures (supplemental data). The specific activity of the administered tracer (for in vitro, in vivo, and stability studies) was in the range of 2–5 MBq/ μg of H_2ATSM precursor.

$^{64}\text{Cu}(\text{II})$ -acetate was administered in physiological saline.

Cell Culture and In Vitro Hypoxia Selectivity

EMT6 and HT1080 cells were obtained from American Type Culture Collection and used within 6 months of resuscitation from frozen stock. Cells were regularly tested to ensure the absence of *Mycoplasma* contamination (MycoAlert; Lonza). Cell morphology was regularly checked to ensure the absence of cross-contamination of cell lines. Cells were grown as monolayers in Dulbecco's modified Eagle's medium, pH 7.4 (Sigma Aldrich) supplemented with 10% fetal bovine serum (HyClone), L-glutamine (2 mM), penicillin (100 units/mL), and streptomycin (100 $\mu\text{g}/\text{mL}$) (Sigma Aldrich). Cells were maintained at 37°C in a 5% CO_2 humidified atmosphere and grown to approximately 95% confluence.

Oxygen-dependent cellular retention assays were conducted in cell suspensions (1×10^6 cells/mL) under normoxic (75% N_2 , 20% O_2 , 5% CO_2) or anoxic (corresponding to severe hypoxia, 95% N_2 , 5% CO_2) conditions as described previously (22–24).

Animal Model, Anesthesia, and Tissue Oxygen Modulation

All animal experiments and protocols were reviewed and performed in accordance with U.K. Home Office in accordance with the Animals Scientific Procedures Act of 1986 (U.K.) and Oxford University regulations. Tumor and normal tissue uptake of ^{64}Cu compounds was determined in female CBA mice (17–20 g) (Charles River) bearing CaNT xenografts. The murine adenocarcinoma (CaNT) tumor line cannot be grown ex vivo. Fifty microliters of a crude cell suspension, prepared by mechanical dissociation of an excised CaNT tumor from a donor animal, were injected. Imaging was performed when tumors had reached approximately 6–8 mm in diameter. The EMT6 tumor model was generated as described previously (23).

Anesthesia was induced and maintained using isoflurane in room air or in oxygen (60% or 100%). Nonanesthetized mice for dissection-only controls were kept in room air or a 60% oxygen or 100% oxygen atmosphere. All animals were maintained in the specified gas mixture

for 30 min before ^{64}Cu -acetate or ^{64}Cu -ATSM injection (intravenous) and then until sacrifice. The hypoxic status of the tumors was confirmed using both the OxyLite probe (Oxford Optronix Ltd.) and EF5 immunohistochemistry as described below.

PET Imaging, Biodistribution, and Blood Speciation Studies

PET imaging was performed using the Inveon PET/CT system (Siemens Preclinical Solutions). Mice were anesthetized, and a cannula was inserted into the lateral tail vein. After the attenuation CT scan, 10 MBq of ^{64}Cu -ATSM or ^{64}Cu -acetate (both in 0.9% saline, pH 7.0) were administered as a bolus injection over 1 s (blood was not aspirated back into the syringe), and 2-h whole-body dynamic images were acquired. Throughout the imaging session, mice were maintained at 37°C, and respiration rate was monitored (60–100 respirations/min). Image analysis was performed using the Inveon Research Workplace software (version 2.2; Siemens Preclinical Solutions).

Immediately after imaging, mice were sacrificed, and organs, tissues, and tumor were removed, washed, and weighed. The blood was collected and weighed. The radioactivity of the samples was counted using an auto γ -counting system (Wizard; Perkin Elmer). The amount of radioactivity in the organs and tissues was calculated as percentage of the injected dose per gram: $[(\text{activity}_{\text{tissue}})/(\text{weight}_{\text{tissue}} \times \text{activity}_{\text{injected}}) \times 100]$. The remainder of the animal was discarded. To avoid any confounding effects of anesthesia, dissection experiments were repeated after sacrifice of mice that had not experienced anesthesia or imaging.

For in vivo blood speciation studies, female, non-tumor-bearing CBA mice (to exclude the effect of the tumor) were injected with ^{64}Cu -ATSM or ^{64}Cu -acetate. Blood samples (~800 μL) were collected at various time points (5–120 min after injection, 2 animals per time point) by heart puncture into heparin-coated tubes. The amount of intact ^{64}Cu -copper complex in the blood was determined via the octanol-extraction method (25,26).

For serum analysis, the vials were spun (4,000 rpm, 4°C, 5 min), and the serum plasma was separated from the red blood cell fraction before being analyzed as referenced below (detailed procedures are given in the supplemental data). Serum binding and stability were determined by the ethanol precipitation method as previously described (24,27).

For in vitro incubations, fresh blood/serum was obtained from mice in an identical manner, incubated with approximately 0.1 MBq of ^{64}Cu -ATSM or ^{64}Cu -acetate, and treated as described for samples from in vivo blood speciation analysis.

Autoradiography and Immunohistochemistry

Tumor hypoxia was confirmed by immunohistologic staining for EF5 (2-(2-nitro-1*H*-imidazol-1-yl)-*N*-(2,2,3,3,3-pentafluoropropyl)-acetamide). For EF5 studies, mice were administered 10 mM EF5 in 0.9% saline intravenously 2 h before tumor excision (EF5 was obtained from Dr. Cameron Koch, University of Pennsylvania (28)). To determine the correlation between ^{64}Cu -ATSM or ^{64}Cu -acetate uptake and hypoxia, tumor slices were analyzed by both autoradiography and EF5 immunohistochemistry (29). Object-based overlap between both modalities was determined by first coregistering autoradiography and fluorescence microscopy images using a rigid transformation. Then, Manders' overlap coefficients (M1) were calculated using the JACoP plug-in for Image J (methods of Manders for spatial intensity correlation analysis with Costes method for automatic thresholding). An in-depth description of JACoP methodology is given in Bolte and Cordelières (30) and in the supplemental data.

Statistical Methods

In vitro cell uptake, in vivo tumor uptake, and in vivo correlation of immunohistochemistry versus autoradiography for all tested

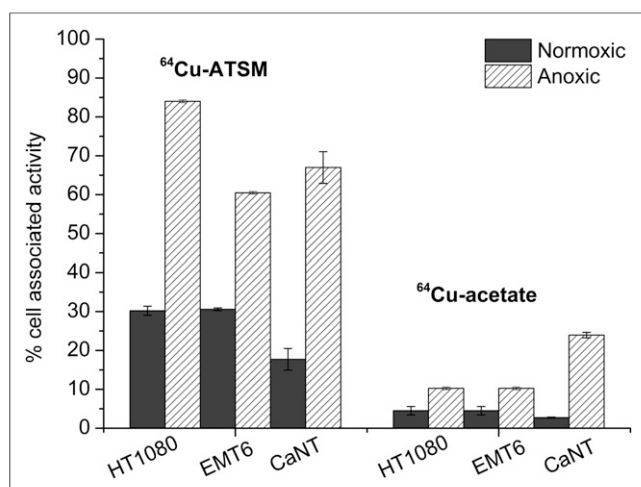


FIGURE 1. In vitro cellular retention of radioactivity at 30 min after incubation under normoxic or anoxic conditions. Experiments were performed in HT1080 and EMT6 cell lines. CaNT cells cannot be cultured in vitro, and assays were conducted on CaNT cells excised from in vivo tumors.

compounds were compared using Graphpad Prism (GraphPad Software Inc.) by 1-way parametric ANOVA with the Tukey adjustment for multiple comparisons ($P < 0.05$). All other statistical comparisons were made using a Student t test ($P < 0.05$). No significant differences were reported when P values were greater than 0.05.

RESULTS

In Vitro Cellular Retention Assays

The radiocopper retention of ⁶⁴Cu-ATSM or ⁶⁴Cu-acetate in vitro by HT1080 and EMT6 cell suspensions was assessed after 30-min incubation under normoxic or anoxic conditions as previously described (Fig. 1) (22,23,31). The radiocopper from ⁶⁴Cu-ATSM was retained in an oxygen-dependent fashion in both cell lines. ⁶⁴Cu-acetate showed low overall cellular retention in both HT1080 and EMT6 cells, with some oxygen dependence in HT1080 cells ($P > 0.05$) and significant ($P < 0.0001$) oxygen

dependence in EMT6 cells under severe hypoxia. This has not previously been reported, probably because of the low overall uptake masking any increases in retention under hypoxia. ⁶⁴Cu-ATSM was also retained to a greater extent in hypoxia than normoxia in a CaNT cell suspension, consistent with the hypoxia selectivity previously reported. Because these cells cannot be grown in vitro, the cell suspensions for these assays were prepared from an excised tumor grown in vivo. Interestingly in these cells, grown in a chronic hypoxic environment, ⁶⁴Cu-acetate showed a larger selectivity for hypoxia than in EMT6 or HT1080.

In Vivo Biodistribution Comparison of ⁶⁴Cu-Acetate and ⁶⁴Cu-ATSM

Before embarking on the in vivo studies, we investigated the reproducibility of hypoxia in mouse tumor models using immunohistochemistry staining for the hypoxia marker EF5. After looking at several tumor lines, we found that CaNT xenografts consistently have significant hypoxic content and little necrosis. EMT6 tumors are also widely used in hypoxia research and were included to provide a point of comparison with results published previously (23,32,33). The in vitro results above suggested that ⁶⁴Cu-acetate would show low uptake and little hypoxia selectivity in vivo and might serve as a control for copper metabolism. This experiment does not appear to have been done previously. In syngeneic mice bearing CaNT tumors, ⁶⁴Cu-ATSM and ⁶⁴Cu-acetate had similar biodistributions at 15 min after injection; however, the tumor-to-muscle ratio for the acetate salt was higher than for the copper complex (Table 1). At 2 h after injection, ⁶⁴Cu-acetate and ⁶⁴Cu-ATSM resulted in broadly similar tumor-to-muscle ratios (7.35 ± 1.13 and 9.93 ± 0.79 , respectively), and both were cleared quickly from the blood with hepatobiliary excretion. The biodistributions for both complexes were similar after 16 h.

The EMT6 tumor xenografts had a tumor-to-muscle-ratio of 9.8 ± 0.63 for ⁶⁴Cu-ATSM, and this was slightly lower (7.9 ± 0.77) for ⁶⁴Cu-acetate at 2 h after injection (full biodistribution data are given in the supplemental data). Dynamic PET scans from 0 to 2 h using ⁶⁴Cu-ATSM and ⁶⁴Cu-acetate in both CaNT- and EMT6 tumor-bearing mice show remarkably similar kinetic behavior, each reaching a steady state at approximately 100 min with similar biodistributions (Fig. 2). It was also notable that

TABLE 1
Biodistribution Data for ⁶⁴Cu-ATSM and ⁶⁴Cu-Acetate in CBA Mice Bearing CaNT Tumors

Organ	⁶⁴ Cu-ATSM (15 min)	⁶⁴ Cu-acetate (15 min)	⁶⁴ Cu-ATSM (120 min)	⁶⁴ Cu-acetate (120 min)	⁶⁴ Cu-ATSM (16 h)	⁶⁴ Cu-acetate (16 h)
Blood	0.61 ± 0.06	0.79 ± 0.06	1.09 ± 0.01	1.28 ± 0.40	1.58 ± 0.16	1.57 ± 0.13
Tumor	0.75 ± 0.10	1.28 ± 0.13	2.41 ± 0.59	2.76 ± 0.63	1.32 ± 0.09	1.28 ± 0.07
Muscle	0.32 ± 0.02	0.27 ± 0.03	0.33 ± 0.05	0.28 ± 0.07	0.20 ± 0.02	0.22 ± 0.01
Stomach	2.91 ± 0.19	2.47 ± 0.21	8.13 ± 3.62	6.67 ± 2.10	3.50 ± 0.50	2.47 ± 0.27
Small intestine	1.29 ± 0.15	1.99 ± 0.22	5.44 ± 0.89	7.02 ± 1.34	4.91 ± 0.63	4.05 ± 0.52
Large intestine	0.47 ± 0.07	0.14 ± 0.01	10.54 ± 1.5	6.27 ± 2.50	7.08 ± 0.36	7.22 ± 0.37
Spleen	1.06 ± 0.06	1.53 ± 0.21	1.54 ± 0.14	2.66 ± 1.01	3.10 ± 0.34	4.19 ± 0.52
Liver	3.61 ± 0.35	4.34 ± 0.57	7.36 ± 0.76	9.93 ± 1.75	9.19 ± 0.90	10.00 ± 1.13
Kidneys	6.20 ± 0.48	4.96 ± 0.43	5.15 ± 0.60	5.60 ± 0.91	7.72 ± 0.70	5.22 ± 0.52
Heart	0.87 ± 0.05	0.79 ± 0.02	1.73 ± 0.32	2.15 ± 1.22	3.30 ± 0.28	2.97 ± 0.20
Lungs	3.21 ± 0.46	4.09 ± 0.38	5.60 ± 0.44	6.44 ± 1.62	7.83 ± 0.77	6.98 ± 0.69
Tumor-to-muscle ratio	2.32 ± 0.19	4.72 ± 0.37	7.35 ± 1.13	9.93 ± 0.79	6.48 ± 0.56	5.88 ± 0.51

Data are percentage injected dose per gram \pm SD.

Awake data, for anesthetized animals, is provided in the supplemental data.

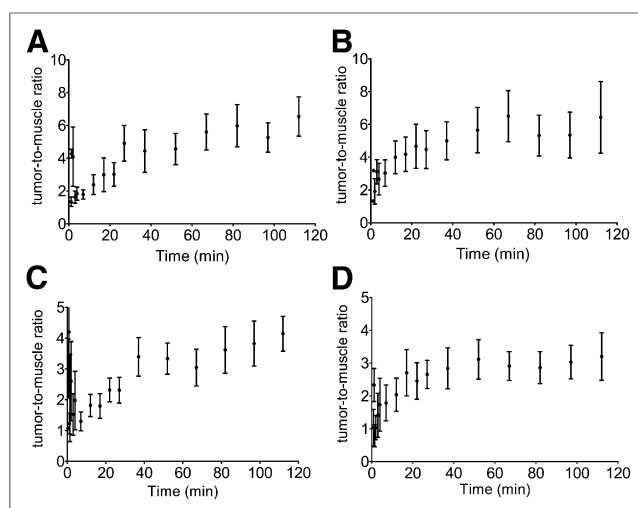


FIGURE 2. Changes in tumor-to-muscle ratios from 0 to 120 min after injection of ^{64}Cu -ATSM ([A] CaNT, [C] EMT6 tumors) and ^{64}Cu -acetate ([B] CaNT, [D] EMT6 tumors) in anesthetized tumor-bearing mice. Time-activity curves were created using volumes of interest composed of several manually defined regions of interest covering target area (tumor tissue, muscle tissue).

tumor-to-muscle ratios for ^{64}Cu -ATSM and ^{64}Cu -acetate were lower for whole-animal imaging (animals dissected after imaging) than for the dissection-only (awake state, that is, no anesthesia) data in both tumor lines. Thus, the effect of anesthesia on tumor uptake of ^{64}Cu -acetate mirrors the effect previously observed for ^{64}Cu -ATSM (34).

Correlation Between Hypoxia and Autoradiography at 15 Minutes, 2 Hours, and 16 Hours After Injection

To determine whether intratumoral ^{64}Cu was distributed preferentially in hypoxic areas, autoradiography of tumors after ^{64}Cu -ATSM and ^{64}Cu -acetate administration was compared with EF5 immunohistochemical staining to identify hypoxic areas. In the reported literature, the correlation of radioactivity from ^{64}Cu -ATSM with hypoxia depended on tumor type and for some was only significant at time points 16–20 h after injection (12,14). Because in the clinical setting ^{64}Cu -ATSM images are commonly acquired between 0 and 60 min after injection (3,35,36), we examined CaNT tumors at 15 min, 2 h, and 16 h after ^{64}Cu -ATSM, ^{64}Cu -acetate, and ^{18}F -MISO administration. The spatial correlation of activity from ^{64}Cu -ATSM, ^{64}Cu -acetate, and ^{18}F -MISO with EF5 distribution was quantified by coregistering the autoradiography and fluorescence microscopy images and obtaining correlation coefficients (Fig. 3). Full biodistribution data, autoradiographs, and EF5 immunofluorescence microscopy images are shown in the supplemental data. These data confirm the presence of hypoxia in these tumors. As expected, a significant positive correlation was found between ^{18}F -MISO and EF5 at 2 h after injection. However, little or no spatial correlation between ^{64}Cu distribution and zones of hypoxia, as defined by EF5 immunohistochemistry, was apparent for either ^{64}Cu -ATSM or ^{64}Cu -acetate at 15 min or 2 h, in contrast to the excellent correlation for ^{18}F -MISO. A stronger correlation was found for ^{64}Cu -ATSM at 16 h, in agreement with previous reports (10,13,14). A similar correlation was found at 16 h also with ^{64}Cu -acetate. Thus, the tumor uptake of ^{64}Cu -ATSM and ^{64}Cu -acetate correlates with tumor hypoxia at 16 h but not at 15 min or 2 h.

Oxygen-Dependent Tumor Uptake of ^{64}Cu -ATSM and ^{64}Cu -Acetate

Tumor oxygenation in vivo can be altered by changing the inhaled oxygen content. For example, Lewis et al. showed that tumor retention of ^{64}Cu using ^{64}Cu -ATSM decreased when animals were breathing 100% oxygen as opposed to air, consistent with the decreased tumor hypoxia (37). To perform analogous experiments but to reduce the potential physiological effects of hyperoxia, we also examined the effect of breathing 60% oxygen on tracer retention in tumors. As depicted in Figure 4 and the supplemental data (Supplemental Table 2), the tumor-to-muscle ratios and tumor uptake of both ^{64}Cu -ATSM and ^{64}Cu -acetate were significantly reduced at 2 h after injection in tumors in animals breathing 100% or 60% O_2 , compared with animals breathing room air. Additionally, anesthetized animals had reduced tumor-to-muscle ratios and tumor uptake of ^{64}Cu -ATSM and ^{64}Cu -acetate, compared with unanesthetized animals. There was decreased tumor uptake of both ^{64}Cu -ATSM and ^{64}Cu -acetate after inhalation of O_2 regardless of the anesthesia regime. All these results are consistent with reduced hypoxia after breathing increased levels of oxygen (34), although copper uptake levels may be influenced by acute changes in tumor blood flow caused by both anesthesia and a change in inhaled oxygen concentration. At the time examined, the radiocopper is not localized in areas of strong hypoxia as delineated by immunohistochemistry. The decrease in tumor retention was more pronounced for ^{64}Cu -acetate than ^{64}Cu -ATSM (34). Muscle retention was unaffected by the inhaled gas. Thus, the effect of reducing copper retention by increasing oxygen content in breathed gas is similar for ^{64}Cu -ATSM and ^{64}Cu -acetate.

^{64}Cu Speciation In Vitro and In Vivo in Blood

The similar biodistributions of ^{64}Cu -acetate and ^{64}Cu -ATSM raised the possibility that a proportion of the copper available for tumor uptake is no longer intact ^{64}Cu -ATSM. To study the copper species present in the blood, we used a previously established ethanol-extraction/-precipitation method (24,27). Ethanol is added to precipitate the proteins present before the supernatant is

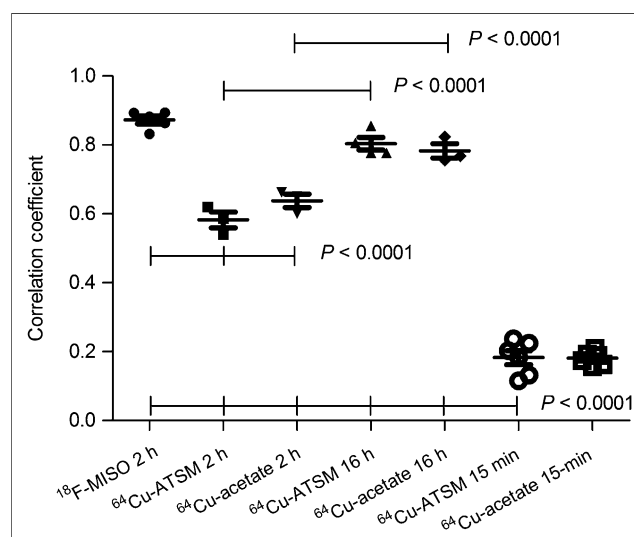


FIGURE 3. Correlation coefficients describing spatial correlation between autoradiography and EF5 immunofluorescence in tumors excised at 15 min, 2 h, or 16 h after injection.

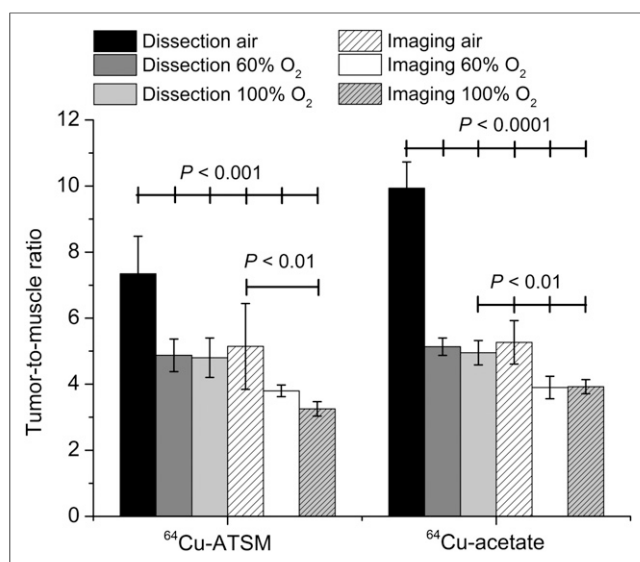


FIGURE 4. Tumor-to-muscle ratios for ^{64}Cu -ATSM and ^{64}Cu -acetate in CaNT tumor-bearing CBA mice as determined by organ dose measurements (percentage injected dose per gram). Mice were either anesthetized with 2% isoflurane/breathing gas (imaging) or awake (dissection) for 120-min biodistribution times. Mice were breathing 100% oxygen, 60% oxygen, or 21% oxygen (room air) before being sacrificed for organ dose measurements.

separated from the proteins. ^{64}Cu -ATSM is stable in serum in vitro. After incubation of ^{64}Cu -acetate with serum in vitro for 2 h, 90% of the activity was associated with the precipitated protein (Fig. 5A). After ^{64}Cu -ATSM was incubated in serum in vitro, 10%–15% of the radioactivity was associated with precipitated protein after 0–2 h and not extracted into ethanol. This was in agreement with the reported results for ^{64}Cu -ATSM and related ^{64}Cu -bis(thiosemicarbazones) after incubation with serum, for which typically approximately 20% of activity was protein-bound (24,27,31). Radio-thin-layer chromatography (radio-TLC) and high-performance liquid chromatography confirmed that the ethanol-extractable radioactivity contained only intact ^{64}Cu -ATSM in agreement with previous in vitro findings (24,27), indicating stability of the complex in serum in vitro.

We then examined the speciation in the blood serum plasma fraction in vivo using the same extraction methods. Ethanol

precipitation and radio-TLC of serum obtained from the blood of mice injected with ^{64}Cu -ATSM or ^{64}Cu -acetate showed high protein binding of radioactivity at all time points (Fig. 5A). Radio-TLC shows that the extractable activity from serum plasma of mice injected with ^{64}Cu -ATSM is primarily in the form of $^{64}\text{Cu}^{2+}$ ion ($R_f = 0$, where R_f refers to the retardation factor; the method is given in the supplemental data). Moreover, the overall amount of solvent-extractable radioactivity from serum after intravenous injection was comparable for ^{64}Cu -ATSM and ^{64}Cu -acetate. This suggests that the protein-bound and solvent-extractable species in the blood in vivo is similar for ^{64}Cu -ATSM and ^{64}Cu -acetate and would be consistent with removal of ^{64}Cu -ATSM by diffusion into the surrounding tissues and organs.

To verify these results, a previously reported octanol-extraction method to examine the amount of intact Cu-ATSM complex in whole blood was also used (25,26). Ionic Cu(II) salts can be extracted into ethanol (ethanol-precipitation method) but do not partition into octanol (octanol-extraction method). After incubation in whole blood in vitro, 85% of ^{64}Cu -ATSM was octanol-extractable at 5 min, decreasing to 53% after 120 min of incubation (Fig. 5B). This percentage is somewhat lower than that observed for incubation in the serum fraction in vitro. This may potentially be explained if Cu-ATSM partitions freely into blood cells, causing partial decomposition in whole blood. Radio-TLC confirmed that the octanol-extractable radioactivity was in the form of ^{64}Cu -ATSM. At 5 min after injection of ^{64}Cu -ATSM into mice, only 23% of the remaining blood radioactivity was octanol-extractable (Fig. 5B), decreasing to 3% after 30 min, which was comparable to the extractable activity observed in mice injected with ^{64}Cu -acetate. The similarity of the data for ^{64}Cu -ATSM and ^{64}Cu -acetate suggests that a proportion of the radiocopper circulating is not intact ^{64}Cu -copper complex but rather serum-bound ^{64}Cu . The identity of the proteins binding the copper or the copper speciation in other compartments has not been established, but the simplest explanation of the similarity of behavior would be that a common copper species in the blood is involved.

DISCUSSION

In both murine xenografts used here, tumor uptake kinetics and biodistributions of ^{64}Cu -ATSM are strikingly similar to those of ^{64}Cu -acetate. Copper uptake at 15 min was slightly higher after the administration of ^{64}Cu -acetate than ^{64}Cu -ATSM, but at 2 and 16 h no significant differences are apparent. In the tumor types we studied, the use of ^{64}Cu -acetate presumably bypasses the redox and dissociative step for Cu-ATSM in tumor retention and thereby selectivity may be significantly determined by copper metabolism.

In vitro incubation in blood or serum did not mimic the rapid decrease in the amount of extractable activity seen in vivo. Therefore, Cu-ATSM removal from the blood likely results from in vivo processes, for instance, the partitioning of Cu-ATSM into the surrounding tissues and organs. This is consistent with our in vivo studies, which show that the remaining blood-born activity is free ^{64}Cu . However, it should be noted that the blood compartment represents only

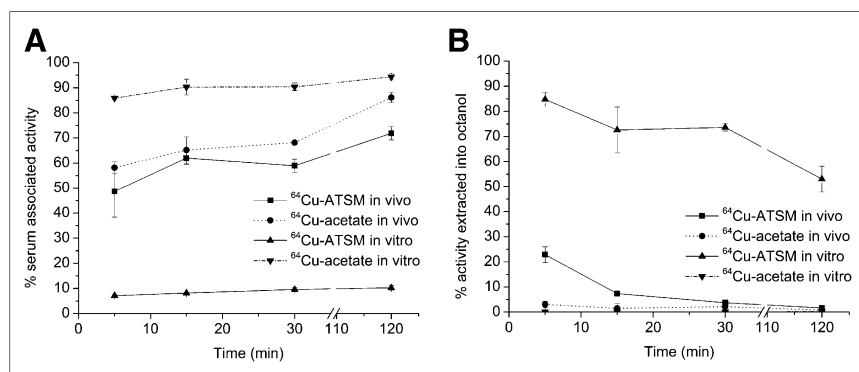


FIGURE 5. In vitro and in vivo stability studies. (A) Percentage of radioactivity remaining bound to serum proteins after ethanol precipitation of serum plasma from in vitro and in vivo blood samples. (B) Percentage of octanol-extractable radioactivity with respect to total blood radioactivity as function of time.

a small proportion of the injected dose (Table 1). Nonetheless, transport of ^{64}Cu or ^{64}Cu -ATSM via the circulation is essential for tumor uptake.

The retention of ^{64}Cu -ATSM by tumors has been shown to correlate with prognosis, and the assumption has been that this results from correlations between tumor hypoxia and copper retention. In vitro examination of the dependence of ^{64}Cu -acetate retention on hypoxia might have led to the prediction that ^{64}Cu -acetate would show little or no hypoxia selectivity in vivo and might serve as a control for copper metabolism. Our results are consistent with those of others, most recently Jorgensen et al., who have also shown that copper accumulates in various murine tumors (18–21). The in vivo distribution and tumor uptake of ^{64}Cu -acetate has not previously been compared directly with that of ^{64}Cu -ATSM. Collectively, our data suggest that the currently proposed redox trapping mechanism might not provide a complete picture, because dismantling of the complex before cell entrance could liberate copper before tumor uptake. At 15 min or 2 h, copper uptake in tumors did not correspond to areas of hypoxia regardless of administration as ^{64}Cu -ATSM or ^{64}Cu -acetate. By 16 h, there was a correlation with areas of hypoxia. Both tracers responded similarly to alterations in the O_2 concentration of respired air, bearing in mind both vascular and O_2 concentrations could play a role in this response. It should finally be noted that copper metabolism in mice has both similarities to and differences from humans, with decreased plasma copper levels in mice, compared with humans. Differences also exist in secondary copper binding proteins but with the liver as a significant copper reservoir in both species (38,39). These data further suggest that the relationship between Cu-ATSM uptake and hypoxia is not entirely direct in vivo, in contrast to results from experiments in tissue culture.

CONCLUSION

Our results serve to emphasize the importance of determining the fate of radiolabeled compounds after administration in vivo and to understand fully the factors governing biodistribution and tumor uptake, thereby facilitating the design of higher performance imaging agents. They suggest that some of the anomalies encountered in the attempts to use ^{64}Cu -ATSM result because radiocopper retention at least partly reflects the processing of copper rather than being solely a direct indicator of hypoxia, particularly at shorter times in the tumor models we have studied here. It is possible that this nonhypoxic tumor retention may provide useful diagnostic information about tumor status. Whatever the ultimate explanation for the radiocopper retention from Cu-ATSM in tumors, it is clear that it still provides unequivocal indication of prognosis for the patient and is therefore clinically relevant.

Our results for the 2 mouse tumor models may not readily be extrapolated to the clinical situation, and there are aspects of a complex mechanism that are not yet understood. However, our findings do raise questions about the currently proposed retention mechanism of Cu-ATSM in vivo, and we hope they may stimulate further preclinical and clinical studies on the relationship between copper metabolism and hypoxia imaging.

DISCLOSURE

The costs of publication of this article were defrayed in part by the payment of page charges. Therefore, and solely to indicate this

fact, this article is hereby marked “advertisement” in accordance with 18 USC section 1734. This work was funded by CRUK and ESPRC through the Oxford Cancer Imaging Centre (C5255/A10339) and funded by CRUK (C5255/A12678, C14521/A6245, and C5255/A8591), GSK, the Gray Laboratory Research Trust (Prof. P. Wardman), OCIC, and the NIHR Oxford Biomedical Research Centre. No other potential conflict of interest relevant to this article was reported.

ACKNOWLEDGMENTS

We thank Drs. Hartmuth Kolb and Jerome Declercq and Siemens Molecular for support of this project. Dr. Romain Bejot and Dr. Laurence Carroll are gratefully acknowledged for assistance with early stages. We thank Dr. Danny Allen for assisting image registration and Dr. Sally Hill, Dr. Nadia Falzone, and Sabira Yameen for technical assistance with in vivo and in vitro biologic work. We thank Prof. Benjamin G. Davis and Prof. Christopher J. Schofield for helpful discussions.

REFERENCES

- Carlin S, Humm JL. PET of hypoxia: current and future perspectives. *J Nucl Med*. 2012;53:1171–1174.
- Fujibayashi Y, Taniuchi H, Yonekura Y, et al. Copper-62-ATSM: a new hypoxia imaging agent with high membrane permeability and low redox potential. *J Nucl Med*. 1997;38:1155–1160.
- Vävere AL, Lewis JS. Cu-ATSM: a radiopharmaceutical for the PET imaging of hypoxia. *Dalton Trans*. 2007;4893–4902.
- Wood KA, Wong WL, Saunders MI. [^{64}Cu]diacetyl-bis(*N* 4-methyl-thiosemicarbazone): a radiotracer for tumor hypoxia. *Nucl Med Biol*. 2008;35:393–400.
- Obata A, Yoshimi E, Waki A, et al. Retention mechanism of hypoxia selective nuclear imaging/radiotherapeutic agent Cu-diacetyl-bis(*N*4-methylthiosemicarbazone) (Cu-ATSM) in tumor cells. *Ann Nucl Med*. 2001;15:499–504.
- Maurer RI, Blower PJ, Dilworth JR, et al. Studies on the mechanism of hypoxic selectivity in copper bis(thiosemicarbazone) radiopharmaceuticals. *J Med Chem*. 2002;45:1420–1431.
- Holland JP, Green JC, Dilworth JR. Probing the mechanism of hypoxia selectivity of copper bis(thiosemicarbazone) complexes: DFT calculation of redox potentials and absolute acidities in solution. *Dalton Trans*. 2006;783–794.
- Holland JP, Barnard PJ, Collison D, et al. Spectroelectrochemical and computational studies on the mechanism of hypoxia selectivity of copper radiopharmaceuticals. *Chem Eur J*. 2008;14:5890–5907.
- Holland JP, Giansiracusa JH, Bell SG, et al. In vitro kinetic studies on the mechanism of oxygen-dependent cellular uptake of copper radiopharmaceuticals. *Phys Med Biol*. 2009;54:2103–2119.
- Yuan H, Schroeder T, Bowsher JE, et al. Intertumoral differences in hypoxia selectivity of the PET imaging agent ^{64}Cu (II)-diacetyl-bis(*N*4-methylthiosemicarbazone). *J Nucl Med*. 2006;47:989–998.
- Burgman P, O'Donoghue JA, Lewis JS, et al. Cell line-dependent differences in uptake and retention of the hypoxia-selective nuclear imaging agent Cu-ATSM. *Nucl Med Biol*. 2005;32:623–630.
- O'Donoghue JA, Zanzonico P, Pugachev A, et al. Assessment of regional tumor hypoxia using ^{18}F -fluoromisonidazole and ^{64}Cu (II)-diacetyl-bis(*N*4-methylthiosemicarbazone) positron emission tomography: comparative study featuring microPET imaging, P2 probe measurement, autoradiography, and fluorescent microscopy in the R3327-AT and FaDu rat tumor models. *Int J Radiat Oncol Biol Phys*. 2005;61:1493–1502.
- Matsumoto K, Szajek L, Krishna MC, et al. The influence of tumor oxygenation on hypoxia imaging in murine squamous cell carcinoma using [^{64}Cu]Cu-ATSM or [^{18}F]fluoromisonidazole positron emission tomography. *Int J Oncol*. 2007;30:873–881.
- Dence CS, Ponde DE, Welch MJ, Lewis JS. Autoradiographic and small-animal PET comparisons between ^{18}F -FMISO, ^{18}F -FDG, ^{18}F -FLT and the hypoxic selective ^{64}Cu -ATSM in a rodent model of cancer. *Nucl Med Biol*. 2008;35:713–720.
- Vävere AL, Lewis JS. Examining the relationship between Cu-ATSM hypoxia selectivity and fatty acid synthase expression in human prostate cancer cell lines. *Nucl Med Biol*. 2008;35:273–279.
- Liu J, Hajibeigi A, Ren G, et al. Retention of the radiotracers ^{64}Cu -ATSM and ^{64}Cu -PTSM in human and murine tumors is influenced by mdrl protein expression. *J Nucl Med*. 2009;50:1332–1339.

17. Dearling JIJ, Packard AB. Some thoughts on the mechanism of cellular trapping of Cu(II)-ATSM. *Nucl Med Biol*. 2010;37:237–243.
18. Peng F, Liu J, Wu JS, Lu X, Muzik O. Mouse extrahepatic hepatoma detected on MicroPET using copper (II)-64 chloride uptake mediated by endogenous mouse copper transporter 1. *Mol Imaging Biol*. 2005;7:325–329.
19. Peng F, Lu X, Janisse J, Muzik O, Shields AF. PET of human prostate cancer xenografts in mice with increased uptake of $^{64}\text{CuCl}_2$. *J Nucl Med*. 2006;47:1649–1652.
20. Zhang H, Cai H, Lu X, et al. Positron emission tomography of human hepatocellular carcinoma xenografts in mice using copper (II)-64 chloride as a tracer. *Acad Radiol*. 2011;18:1561–1568.
21. Jørgensen JT, Persson M, Madsen J, Kjær A. High tumor uptake of ^{64}Cu : implications for molecular imaging of tumor characteristics with copper-based PET tracers. *Nucl Med Biol*. 2013;40:345–350.
22. Carroll L, Bejot R, Hueting R, et al. Orthogonal ^{18}F and ^{64}Cu labelling of functionalized bis(thiosemicarbazonato) complexes. *Chem Commun (Camb)*. 2010;46:4052–4054.
23. Lewis JS, McCarthy DW, McCarthy TJ, et al. Evaluation of ^{64}Cu -ATSM in vitro and in vivo in a hypoxic tumor model. *J Nucl Med*. 1999;40:177–183.
24. Bonnichs PD, Vavere AL, Lewis JS, Dilworth JR. In vitro and in vivo evaluation of bifunctional bithiosemicarbazone ^{64}Cu -complexes for the positron emission tomography imaging of hypoxia. *J Med Chem*. 2008;51:2985–2991.
25. Mathias CJ, Bergmann SR, Green MA. Development and validation of a solvent extraction technique for determination of Cu-PTSM in blood. *Nucl Med Biol*. 1993;20:343–349.
26. Lewis JS, Herrero P, Sharp Terry L, et al. Delineation of hypoxia in canine myocardium using PET and copper(II)-diacetyl-bis(N(4)-methylthiosemicarbazone). *J Nucl Med*. 2002;43:1557–1569.
27. McQuade P, Martin KE, Castle TC, et al. Investigation into ^{64}Cu -labeled bis(selenosemicarbazone) and bis(thiosemicarbazone) complexes as hypoxia imaging agents. *Nucl Med Biol*. 2005;32:147–156.
28. Koch CJ. EF5 Procedure Manual. <http://www.hypoxia-imaging.org/v2/methods/ef5manual.htm>. Accessed November 7, 2013.
29. Lee J, Siemann DW, Koch CJ, Lord EM. Direct relationship between radiobiological hypoxia in tumors and monoclonal antibody detection of EF5 cellular adducts. *Int J Cancer*. 1996;67:372–378.
30. Bolte S, Cordelieres FP. A guided tour into subcellular colocalization analysis in light microscopy. *J Microsc*. 2006;224:213–232.
31. Bonnichs PD, Bayly SR, Theobald MBM, et al. Nitroimidazole conjugates of bis(thiosemicarbazonato) ^{64}Cu (II): potential combination agents for the PET imaging of hypoxia. *J Inorg Biochem*. 2010;104:126–135.
32. Dearling JIJ, Lewis JS, Mullen GED, et al. Copper bis(thiosemicarbazone) complexes as hypoxia imaging agents: structure-activity relationships. *J Biol Inorg Chem*. 2002;7:249–259.
33. Franko AJ. Hypoxic fraction and binding of misonidazole in EMT6/Ed multicellular tumor spheroids. *Radiat Res*. 1985;103:89–97.
34. Kersemans V, Cornelissen B, Hueting R, et al. Hypoxia imaging using PET and SPECT: the effects of anesthetic and carrier gas on [^{64}Cu]-ATSM, [$^{99\text{m}}\text{Tc}$]-HL91 and [^{18}F]-FMISO tumor hypoxia accumulation. *PLoS ONE*. 2011;6:e25911.
35. Holland JP, Lewis JS, Dehdashti F. Assessing tumor hypoxia by positron emission tomography with Cu-ATSM. *Q J Nucl Med Mol Imaging*. 2009;53:193–200.
36. Chia K, Fleming IN, Blower PJ. Hypoxia imaging with PET: which tracers and why? *Nucl Med Commun*. 2012;33:217–222.
37. Lewis JS, Sharp TL, Laforest R, et al. Tumor uptake of copper-diacetyl-bis(n4-methylthiosemicarbazone): effect of changes in tissue oxygenation. *J Nucl Med*. 2001;42:655–661.
38. Gray LW, Kidane TZ, Nguyen A, et al. Copper proteins and ferroxidases in human plasma and that of wild-type and ceruloplasmin knockout mice. *Biochem J*. 2009;419:237–245.
39. Cabrera A, Alonzo E, Sauble E, et al. Copper binding components of blood plasma and organs, and their responses to influx of large doses of ^{65}Cu , in the mouse. *Biometals*. 2008;21:525–543.



The Journal of
NUCLEAR MEDICINE

A Comparison of the Behavior of ^{64}Cu -Acetate and ^{64}Cu -ATSM In Vitro and In Vivo

Rebekka Hueting, Veerle Kersemans, Bart Cornelissen, Matthew Tredwell, Kamila Hussien, Martin Christlieb, Antony D. Gee, Jan Passchier, Sean C. Smart, Jonathan R. Dilworth, Véronique Gouverneur and Ruth J. Muschel

J Nucl Med. 2014;55:128-134.

Published online: December 12, 2013.

Doi: 10.2967/jnumed.113.119917

This article and updated information are available at:
<http://jnm.snmjournals.org/content/55/1/128>

Information about reproducing figures, tables, or other portions of this article can be found online at:
<http://jnm.snmjournals.org/site/misc/permission.xhtml>

Information about subscriptions to JNM can be found at:
<http://jnm.snmjournals.org/site/subscriptions/online.xhtml>

The Journal of Nuclear Medicine is published monthly.
SNMMI | Society of Nuclear Medicine and Molecular Imaging
1850 Samuel Morse Drive, Reston, VA 20190.
(Print ISSN: 0161-5505, Online ISSN: 2159-662X)

© Copyright 2014 SNMMI; all rights reserved.

The logo for the Society of Nuclear Medicine and Molecular Imaging (SNMMI) consists of the letters 'S', 'N', 'M', and 'I' arranged in a 2x2 grid. Each letter is white and set within a red square. To the right of this grid is a vertical line, followed by the text 'SOCIETY OF NUCLEAR MEDICINE AND MOLECULAR IMAGING' in a sans-serif font.
SOCIETY OF
NUCLEAR MEDICINE
AND MOLECULAR IMAGING